

# Study of the cooling of a uniformly heated vertical tube by an ascending flow of air and a falling water film

P. An, J. Li, J.D. Jackson \*

*School of Engineering, Simon Building, The University of Manchester, Oxford Road, Manchester M13 9PL, UK*

## Abstract

An experimental study is reported of the cooling of an electrically heated tube by a flow of air ascending within it in the presence of a thin falling water film. This was produced by spraying jets onto the inside surface of the tube at the top and allowing the water to run down the inside surface. Experiments were performed for a range of values of power input with both naturally induced and forced airflow to examine the influence of water injection temperature and water flow rate on the distribution of temperature along the tube. The results obtained show that when the water is supplied at a temperature of about 20°C, the dominant heat removal mechanism is convective cooling by the falling film. In contrast, when the water is supplied at temperatures of 55°C and above the dominant mechanism is evaporation of water from the surface of the film. A semi-empirical model developed for the purpose of aiding the interpretation of the experimental results reproduced observed behaviour very satisfactorily and enabled a clear picture to be obtained of the extent to which the various mechanisms of heat transfer involved contribute to the removal of heat. © 1999 Elsevier Science Inc. All rights reserved.

## 1. Introduction

This research was initiated as a result of an interest in the problem of passive heat removal by means of naturally induced airflow from the outer surface of the steel containment vessel of a water-cooled nuclear reactor of advanced design. In the arrangement under consideration, air flows upward in a passage between the containment vessel and an outer concrete shell simply as a result of receiving heat from the vessel. Due to the low flow rates which are typical of naturally induced cooling systems, one would not expect to achieve high rates of heat removal by this means. There is, however, an additional reason why the effectiveness of heat transfer might be limited. Depending on the thermal conditions and the geometry of the system, strong interactions between free and forced convection might occur within the airflow. These could lead to a reduction in turbulence production and impairment of heat transfer.

The influence of buoyancy on heat transfer under conditions of turbulent forced flow in vertical tubes has received considerable attention over the years – see for instance Jackson and Hall (1979) and Jackson et al. (1989). In the buoyancy-aided situation (upward flow in a heated tube), the shear force exerted on the flow by the wall can be partly, or even wholly, overcome by the buoyancy of the fluid adjacent to it. As a result, the local shear stress falls steeply with distance from the wall, turbulence production is affected and heat transfer by turbulent diffusion is impaired. The experimental study by Li (1994) of heat transfer to air which was induced naturally through a heated vertical tube has demonstrated that buoy-

ancy-induced impairment of heat transfer can also happen under such conditions (see Jackson et al., 1995). Fig. 1 shows experimental data from Li (1994) for both naturally induced flow and upward forced flow. The results are presented in the form of Nusselt number normalised using the forced convection value evaluated at the flow rate in question, and a buoyancy parameter of the kind proposed by Jackson and Hall, 1979. It can be seen that there is a range of buoyancy parameter within which heat transfer is impaired in relative terms for both the naturally induced flow and forced flow cases. Note also that when presented in this form the two sets of data map onto each other. The results presented are for locations sufficiently downstream that fully developed flow conditions were approached.

One method which has been proposed to overcome the limitations on heat transfer which might be encountered in the nuclear reactor containment cooling application is to enhance the heat removal process by allowing a thin film of water to run down the outer surface of the vessel (see for instance Bruschi and Vijuk, 1991). In the study reported here, experiments have been conducted to evaluate the potential of this approach and also to identify and quantify the mechanisms of heat transfer involved.

The experimental arrangement in the present study consisted of a uniformly heated vertical tube with a flow of air supplied at the bottom which could be either induced naturally or pumped. The reason for studying the forced flow case as well as the naturally-induced one was that in the computational modelling studies undertaken to examine the heat transfer mechanisms involved the flow rate of air was needed as an input parameter. This could not be readily measured under the conditions of the naturally-induced flow experiments.

\* Corresponding author. E-mail: [jdjackson@man.ac.uk](mailto:jdjackson@man.ac.uk).

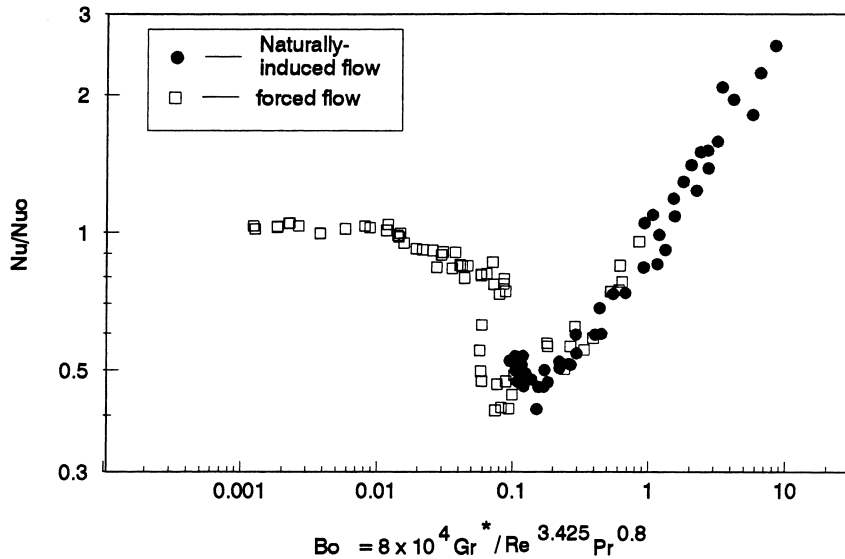


Fig. 1. Relative heat transfer as a function of buoyancy parameter.

## 2. Experimental investigation

### 2.1. Apparatus

Fig. 2 shows the two different experimental arrangements which have been used in the present study. The test section was made from an 8 m length of stainless steel tube, of internal diameter 76 mm and wall thickness 1.9 mm, the uniformity of which had been carefully checked using an ultrasonic thickness gauge. The tube was mounted vertically and the outside was covered with a thick layer of thermal insulation.

Heat was generated within the tube wall by passing electric current through it from a variable voltage AC supply system. Air flowed upwards within the tube in the presence of a thin film of water running down the inside surface. The distribution of temperature along the tube was measured by thermocouples welded to the outside surface at numerous axial locations. At the top of the test section, water was sprayed in a symmetrical manner onto the inside surface of the tube from a centrally positioned multi-jet nozzle so as to produce a uniform film which ran downwards. The injection system could be supplied with water at chosen values of temperature and flow rate. The

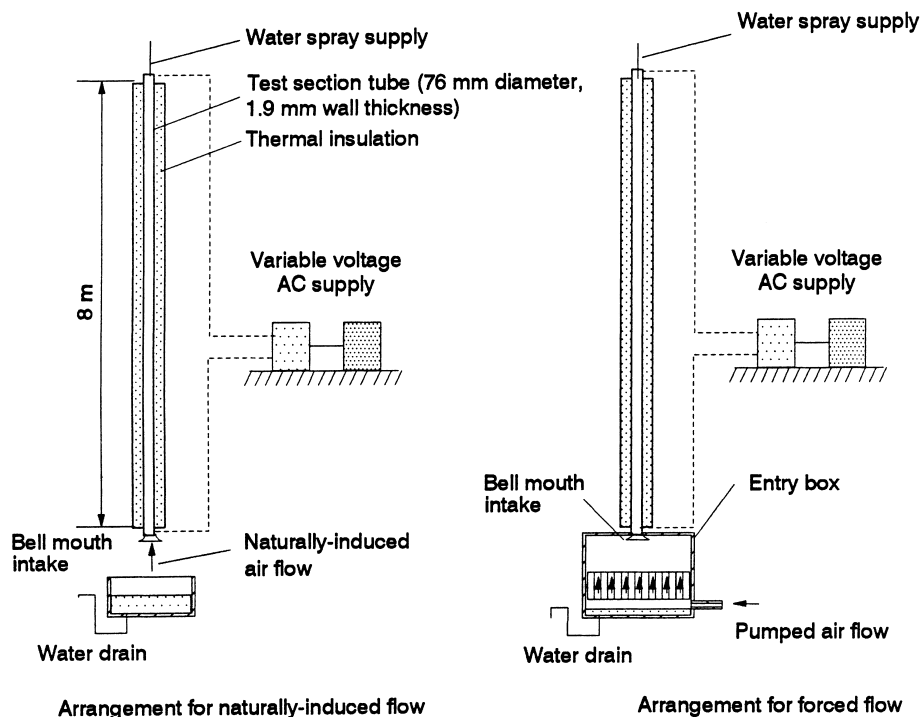


Fig. 2. Test section arrangements.

preheating of the water was achieved by means of electrical immersion heaters located in the supply line and the flowrate was measured using a rotameter.

Air from the laboratory was either induced naturally through the test section, as in the arrangement shown on the left, or was pumped steadily to an entry box which enclosed the bellmouth intake at the bottom of the tube, as shown in the arrangement on the right. In the latter case, the flow rate of air was monitored using a carefully calibrated flowmeter installed in the supply line.

2.2. Experimental procedure and conditions

In the case of experiments with water film cooling, the operating procedure was to begin by injecting water at the top of the test section via the spray nozzle. Once a steady and uniform film had been established, electrical heating was applied to the tube with air flowing upwards within it, either as a result of being pumped (the forced flow case) or simply as a result of it being heated with the tube open at the top and bottom (the naturally-induced case). After a lengthy period of time, during which the temperature distribution along the tube was monitored at regular intervals using an automatic data acquisition system, a steady condition was achieved. Some tests were conducted without water injection (referred to in the text as ‘dry tests’).

The experimental conditions covered were as follows:  
 Electrical power input: 1.35, 3.0, 4.0 and 5.0 kW.  
 Water injection rate: 0.013 and 0.027 kg/s.  
 Water temperature at inlet: 20°C, 40°C, 55°C, 60°C and 70°C.

The air entering the test section was at a temperature of 20°C. In the forced flow experiments, it was supplied at rates of 0.005, 0.010 and 0.015 kg/s. The Reynolds numbers at inlet corresponding to the three quoted air flow rates were 4600, 9200 and 13800.

2.3. Experimental results

2.3.1. Naturally-induced airflow

Figs. 3(a) and (b) shows some results for the case of naturally-induced flow with and without water film cooling for power inputs of 1350 and 3000 W. It can be seen from Fig. 3(a) that the tube wall temperature is significantly reduced as a result of the application of water film cooling. As might have been anticipated, the greatest reduction is obtained with water injected at the lowest temperature (20°C). As the water runs down the tube its temperature rises and it carries with it most of the heat generated within the tube wall. Increasing the injection temperature to 45°C has the effect of changing the heat removal mechanism. In this case the water temperature remains almost constant as it runs down the tube. Water evaporates from the surface of the film and the heat generated in the tube is used to provide the enthalpy of evaporation. Further increase of injection temperature to 70°C leads to even higher rates of evaporation which result in the temperature of the water falling as it runs down the tube.

Fig. 3(b) shows results for an increased power input (3000 W). It can be seen that as a consequence of the development of buoyancy-induced impairment of heat transfer the tube temperature was very non-uniform in the dry test and rose to about 360°C near the top of the test section. This value was close to the operating temperature limit chosen to ensure that

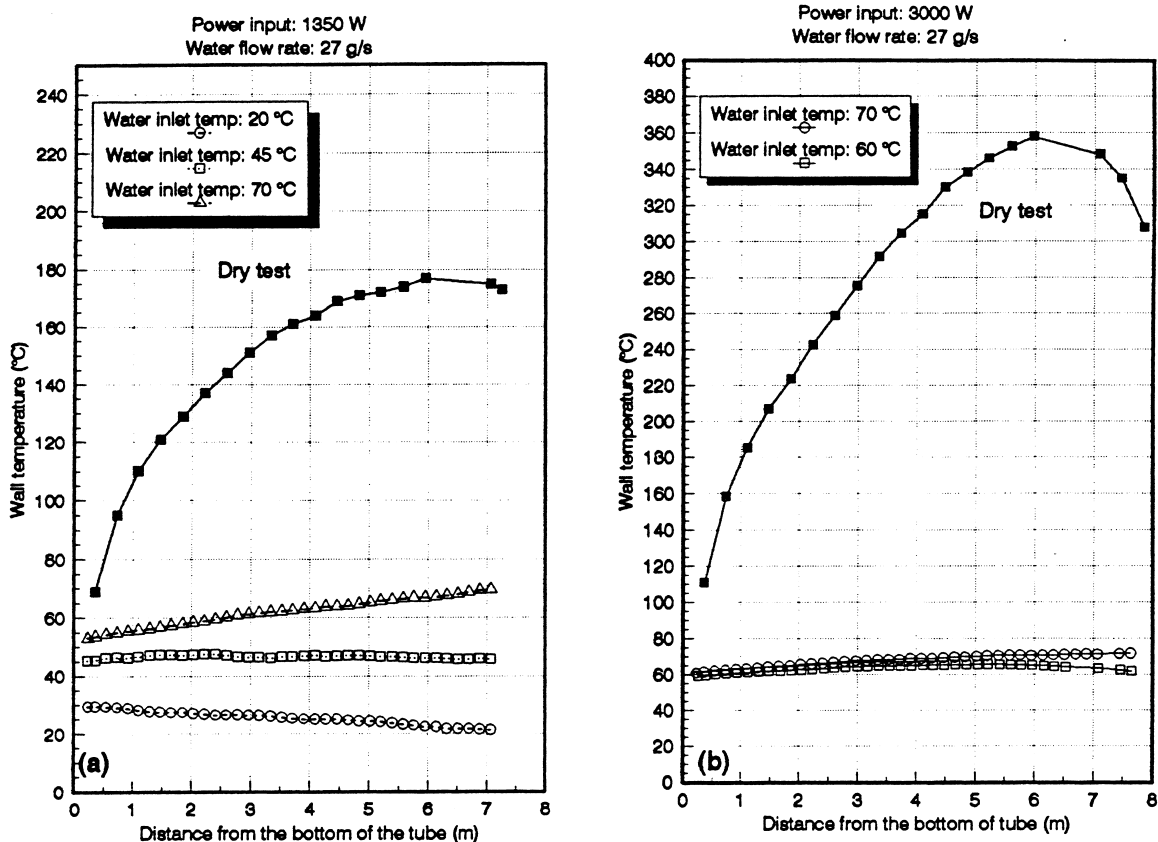


Fig. 3. Tube wall temperature distributions with and without water film cooling for the case of naturally-induced flow.

the test section did not get damaged as a result of being overheated. The application of water film cooling reduced the tube temperature to a uniform value of about 60°C. Again, the mechanism of heat removal was evaporation of water from the surface of the film.

### 2.3.2. Forced airflow

Having clearly demonstrated the beneficial influence of water film cooling under passive conditions (naturally induced airflow), experiments with forced airflow were performed next.

Fig. 4 shows tube wall temperature distributions for forced airflow under dry conditions with power inputs of 1350 and 3000 W. For the lower value of power, the tube reached a temperature of about 300°C near the top with an air flow rate of 0.005 kg/s. In that test, influences of buoyancy were again significant. The developing interaction between free and forced convection is evident from the irregular shape of the tube wall temperature distribution. With a power input of 3000 W the wall temperature reached 300°C for an air flow rate of 0.015 kg/s. Dry tests were not performed with lower flow rates at that power so as to avoid exceeding the test section operating temperature limit. The results shown in Fig. 4 provide a base against which corresponding ones with water film cooling can be compared.

Fig. 5 shows comparisons between results from experiments with and without water film cooling for an airflow rate of 0.015 kg/s with a power input of 1350 W. Results are presented for values of water temperature at inlet of (a) 20°C, (b) 40°C, (c) 55°C and (d) 70°C at two different water flow rates (0.013 and 0.027 kg/s). It can be seen that the behaviour changes markedly as the water temperature at inlet is increased. In all cases, water film cooling causes tube temperature to be greatly reduced.

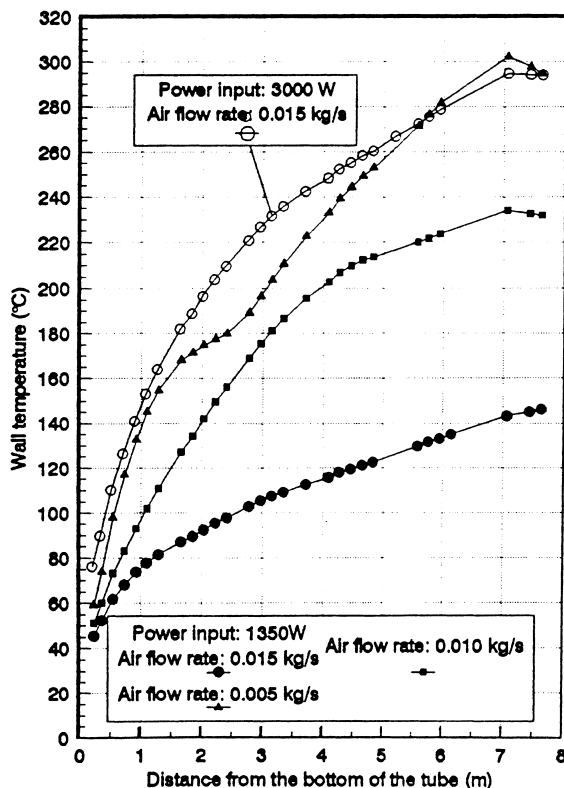


Fig. 4. Tube wall temperature distributions without water film cooling for the case of forced air flow.

From Fig. 5(a) (water injection temperature 20°C) it can be seen that the temperature of the water, which is effectively that of the tube, first rises and then falls as it runs downwards. As one would expect, the rate at which it increases is greater in the case of the lower water flow rate because the heat input from the tube to the water is the same. The eventual fall of temperature is brought about by evaporation of water from the surface of the film. The saturation vapour pressure of water increases strongly with temperature and hence the rate of evaporation is very sensitive to the water temperature. Evaporation is therefore, greatest in the lower part of the tube where the water temperature is highest. Once the effect of heat removal due to evaporation exceeds the rate at which heat is generated within the tube wall, the temperature of the descending water begins to fall. The changeover occurs earlier in the case of the test with the lower water flow rate because the temperature of the water reaches a higher value in that case as a result of the rise of temperature in the upper part of the tube being steeper. The water leaving the bottom of the test section is at a higher temperature than when it was injected at the top and most of the heat generated in the tube wall is carried away by the water passing through the test section. The air/vapour mixture, which rises up within the tube increasing in temperature, leaves at the top carrying some heat with it. In the upper part of the tube the conditions can be such that some of the ascending vapour condenses onto the water film releasing heat as it does. Thus, we see that a variety of heat transfer mechanisms can be involved in the seemingly simple system under consideration here.

Referring next to the results shown in Fig. 5(b), where the water temperature at inlet is 40°C, we see that the behaviour is rather different. The temperature of the descending water varies much less. A small net rise in temperature occurs in the case of the higher water flow rate and there is a small net decrease in the case of the lower water flow rate. Evaporation from the film has a significant effect on heat removal over the whole length of the tube with water injected at this temperature. As one would expect, the extent to which the water is cooled is greater in the case of the lower water flow rate, so the two distributions of tube wall temperature do diverge slightly in the lower part of the test section. However, the influence on tube wall temperature of changing the water flow rate is quite small.

Fig. 5(c) shows results for a water temperature at inlet of 55°C. The trend in terms of increased importance of evaporation with increase of water temperature at inlet is continued. For both the water flow rates covered, the effect of evaporation is to cause the descending water to fall in temperature. Again, the rate at which this occurs is greater for the lower water flow rate. We see that the air/vapour mixture leaving the top of the test section not only takes with it the electrical energy generated within the tube wall but also heat which has been released by the descending water film.

Finally, we consider the results shown in Fig. 5(d) for the highest inlet water temperature (70°C). Here, evaporation is of even greater importance. A steep fall in the temperature of the descending water film is evident, particularly where the temperature of the water is highest near the top of the test section. Again, the effect is greatest in the case of the experiment with the lower water flow rate.

Fig. 6 shows the influence of air flow rate on tube wall temperature for water temperatures at inlet of 20°C, 40°C, 55°C and 70°C with a power input of 1350 W. Three values of airflow rate are covered (0.005, 0.010 and 0.015 kg/s).

For a water temperature at inlet of 20°C, it can be seen from Fig. 6(a) that air flow rate only affects the heat transfer process in the lower part of the tube. There, evaporation from the descending water film begins to be significant. As the

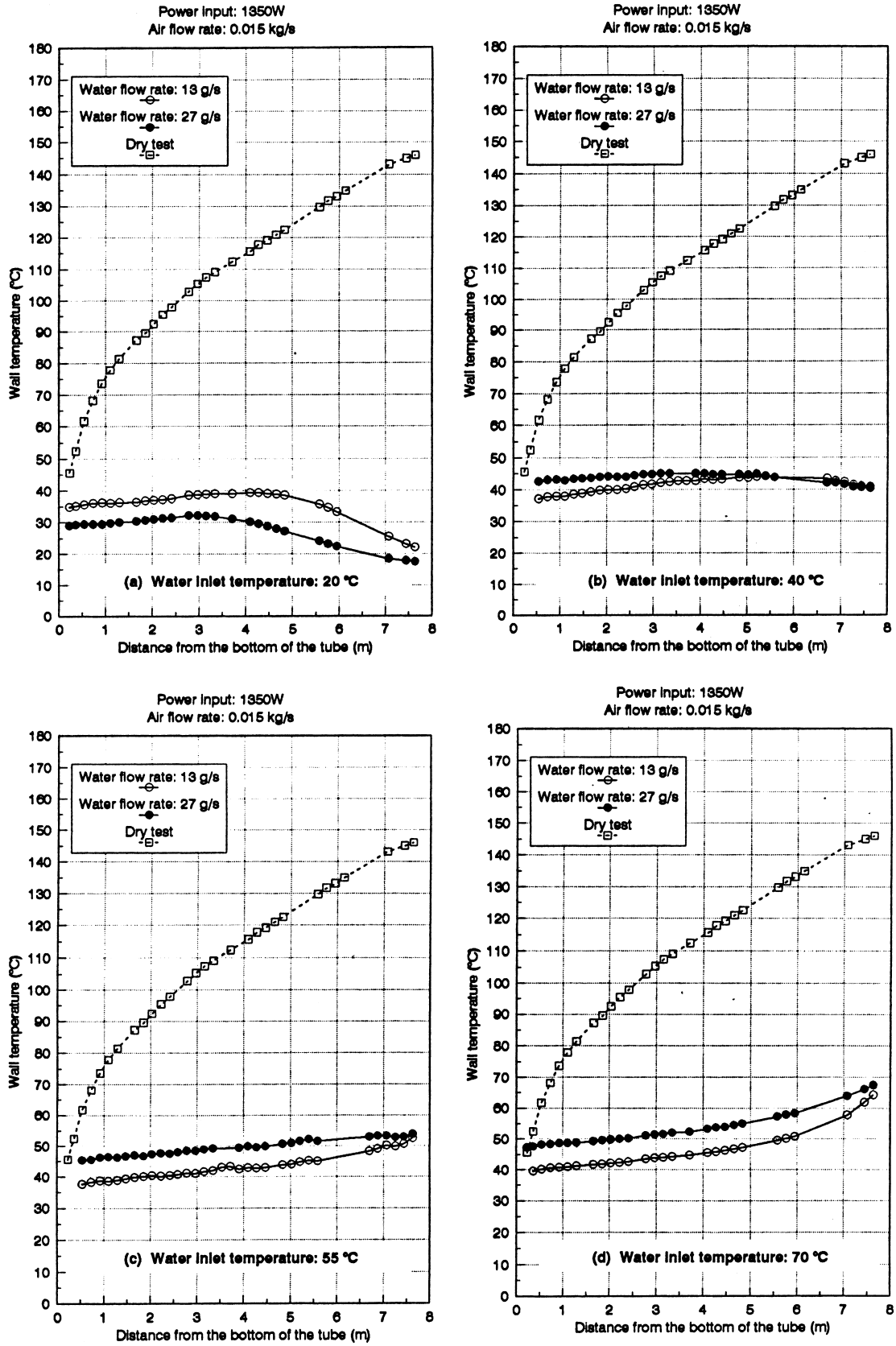


Fig. 5. Tube wall temperature distributions with and without water film cooling – effect of water flow rate.

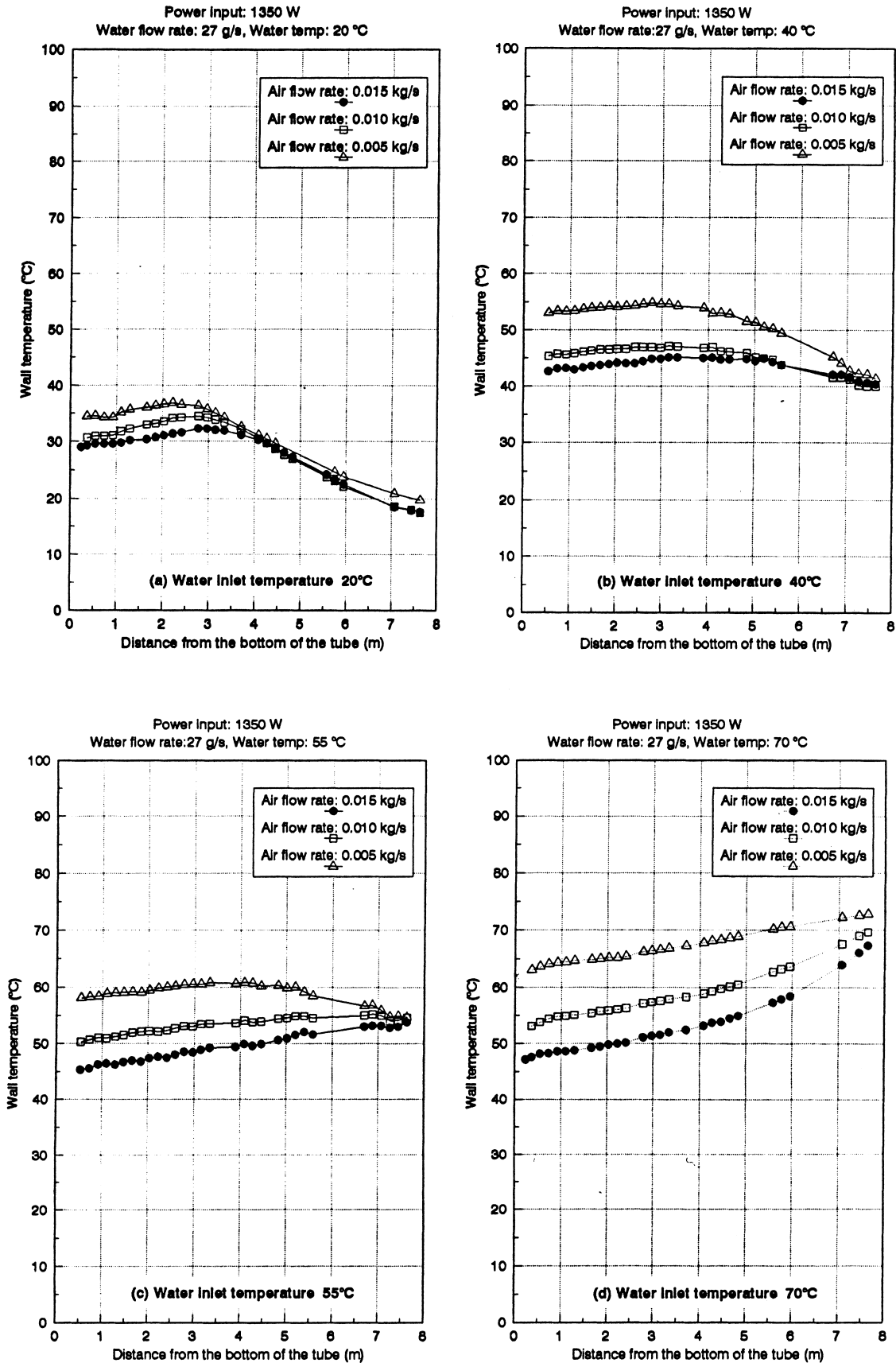


Fig. 6. Tube wall temperature distributions with water film cooling – effect of air flow rate.

airflow rate is reduced, the tube wall temperature has to be higher in order to transfer heat by turbulent convection from the water film into the air/vapour mixture. The effect is most apparent at the lowest airflow rate of 0.005 kg/s. Similar trends with reduction of airflow rate are progressively more and more evident in the case of the corresponding results for inlet water temperatures of 40°C, 55°C and 70°C shown in Fig. 6(b), (c) and (d). The heat transfer mechanisms in the series of experiments presented in Fig. 6 are essentially the same as those described earlier in the discussion of Fig. 5.

Figs. 7 and 8 together provide a picture of what happens as the electrical power input to the tube is increased to 3000 W and then to 5000 W with a fixed value of inlet water temperature of 70°C. Three air flow rates were covered in each case. As in the corresponding case for a power input of 1350 W (Fig. 6(d)), it can be seen that wall temperature is rather dependent on air flow rate and a systematic increase of wall temperature is evident as the air flow rate is reduced. However, the most striking feature of this series of results is that the tube wall temperature only rises by a relatively small amount as the electrical power input is increased by a factor of over three. With a power input of 5000 W the peak value of wall temperature is only ten degrees higher than that for a power input of 1350 W. In each case the dominant heat transfer mechanism is evaporation of water from the descending water film. Not only is heat removed from the tube but the water is also cooled down by a significant amount as it passes through the test section.

The effectiveness of evaporation from the falling water film as a mechanism for heat removal can be seen by comparing the result for a power input of 3000 W shown in Fig. 4 with the

results shown in Fig. 7. It is clear that without water film cooling the tube wall temperature would have been greatly in excess of 300°C for a power input of 5000 W and serious overheating of the test section could have resulted. However, by applying water film cooling with water injected at 70°C, this power can be safely removed.

### 3. Semi-empirical model

#### 3.1. Modelling studies

With a view to reinforcing the interpretation of the experimental results and quantifying the various contributions to heat removal involved, modelling studies were undertaken at two different levels. Computational simulations were performed using an advanced formulation of the combined heat and mass transfer problem involving the numerical solution of the governing differential equations. This work has been reported separately (see He et al., 1998). In addition, the simple semi-empirical model described below was developed.

#### 3.2. Physical system and approach

It is assumed that the tube is perfectly insulated on the outside so that all the heat generated within the tube passes directly to the water which runs down the inside surface under the action of gravity. The water film is assumed to be circumferentially uniform, and to flow without surface ripples in a steady, laminar manner. The basis for this is that the Reynolds number of the film flow, calculated knowing the

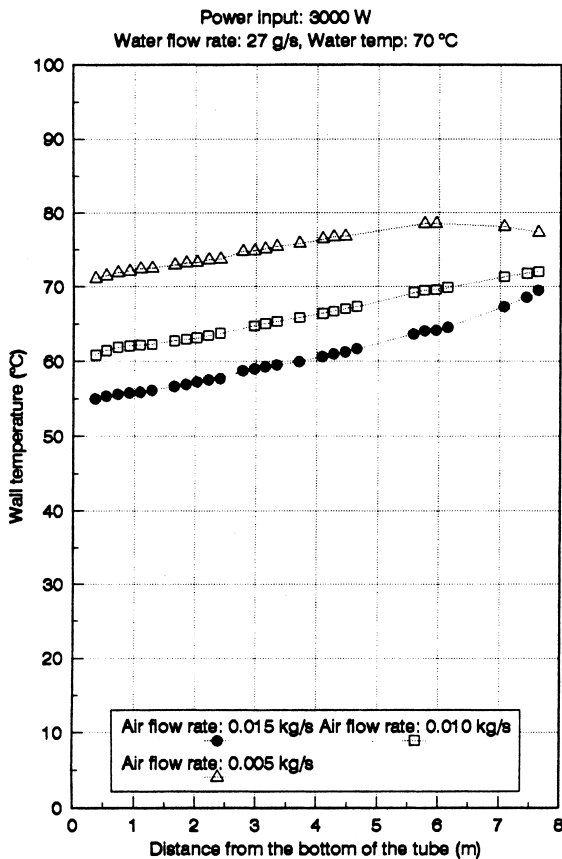


Fig. 7. Tube wall temperature distributions with water film cooling.

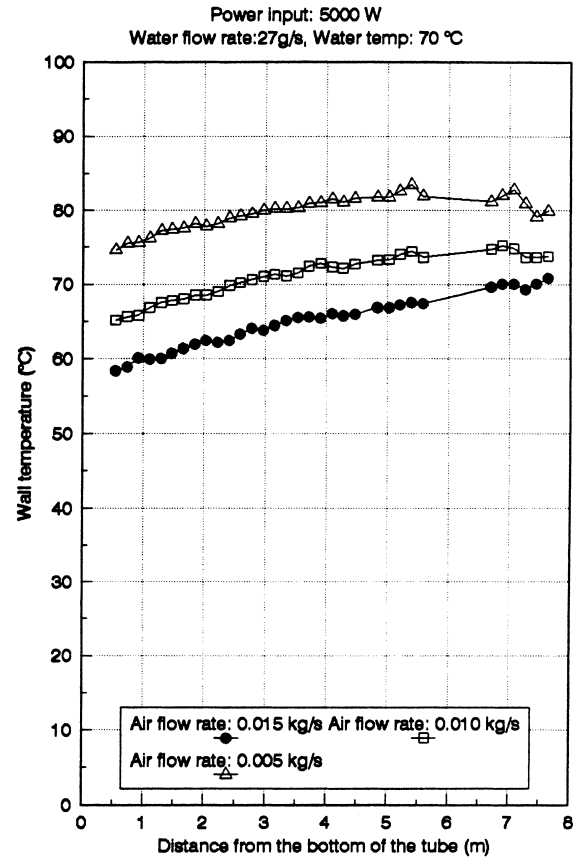


Fig. 8. Tube wall temperature distributions with water film cooling.

mass flow rate of water and utilising the simple analytical solution for steady, fully developed laminar flow of a film of liquid down a vertical surface under the action of gravity, was about 450 for the highest flow rate, considered. This is much less than the critical value of 1500 quoted by Ueda and Tanaka, 1975. The applicability of the solution was tested in the course of the experimental study by determining the velocity with which the water ran down the pipe using a technique which involved marking the incoming water by suddenly introducing salt solution and measuring the time taken for it to arrive at the bottom of the tube where it was detected by an electrical probe. The results obtained by this means were in satisfactory agreement with values calculated using the analytical solution knowing the measured mass flow rate of water.

The test section is considered as  $n$  elements (see Fig. 9). Each element consists of three parts, the wall, the water film and the air/vapour mixture region. The variables for each element are the tube wall temperature  $T_{w,i}$ , the temperature of the water film  $T_{l,i}$  (effectively equal to  $T_{w,i}$ ) the air/vapour mixture temperature  $T_{g,i}$ , and the concentration of vapour in the mixture  $d_{v,i}$ . The mixture velocity  $V_{g,i}$  can be calculated from overall continuity considerations knowing the values of the variables.

The input parameters are the electrical power  $\dot{Q}$  supplied to heat the tube, the water temperature at inlet  $T_{l,n}$  ( $= T_{w,n}$ ), the water injection flow rate  $\dot{m}_l$ , the air flow rate  $\dot{m}_a$ , the air temperature at inlet  $T_a$  ( $= T_{g,o}$ ) and the relative humidity of the air at inlet  $R_h$ .

The mass and energy balance equations are formulated for the water film and air/vapour mixture regions. The well-established empirical correlation of Petukhov et al. (1972) for forced convection in tubes shown below is used to obtain the heat transfer coefficient for the transfer process from the water film to the air/vapour mixture.

$$Nu = \frac{CRePrf/2}{1.07 + \frac{900}{Re} - \frac{0.63}{1+10Pr} + 12.7\sqrt{f/2}(Pr^{2/3} - 1)}$$

in which  $Nu$  is Nusselt number,  $Re$  is Reynolds number,  $Pr$  is Prandtl number,  $C$  is a thermal development factor and  $f$  is friction coefficient.

The thermal development factor is related to Reynolds number and axial location  $x/D$  by

$$C = 1.0 + \frac{0.48}{(x/D)^{0.25}} \left[ 1 + \frac{3600}{Re\sqrt{x/D}} \right] \exp(-0.17x/D).$$

Friction coefficient is related to Reynolds number by

$$f = \frac{1}{4} [1.82 \log_{10}(Re/8)]^{-2} \quad \text{for } 10^4 \leq Re \leq 5 \times 10^6$$

and

$$f = 0.09Re^{-0.25} \quad \text{for } 4000 \leq Re \leq 10^4.$$

The rate of evaporation from the water film is calculated using a mass transfer coefficient obtained utilising the analogy between heat and mass transfer. The calculation is carried out iteratively proceeding from element 1 to element  $n$ , starting by assuming a value for the wall temperature  $T_{w,0}$ . The procedure for a general element  $i$  is as follows.

Assuming  $T_{w,i} = T_{w,i-1}$ ,  $T_{g,i} = T_{g,i-1}$ ,  $d_{v,i} = d_{v,i-1}$  and  $V_{g,i} = V_{g,i-1}$ , the rate of convective heat transfer  $\dot{q}_{lg,i}$ , from the water film to the air/vapour mixture and the rate of evaporation  $\dot{m}_{lg,i}$  are calculated knowing coefficients of heat and mass transfer obtained using the empirical equations for Nusselt and Sherwood number as functions of Reynolds number,  $x/D$  and Prandtl and Schmidt numbers, respectively. The Reynolds number is defined using the relative velocity ( $V_{g,i} - V_{l,i}$ ) with  $V_{l,i}$  being calculated using the analytical solution for the falling film flow with the water properties evaluated at the local temperature  $T_{l,i}$  ( $= T_{w,i}$ ). New values of  $T_{w,i}$ ,  $T_{g,i}$ ,  $d_{v,i}$  and  $V_{g,i}$  are calculated using the energy and mass balance equations for the water film and air/vapour mixture regions and overall continuity considerations. The procedure is repeated iteratively until the values of the variables converge to within a specified accuracy. By proceeding in this manner from element 1 to

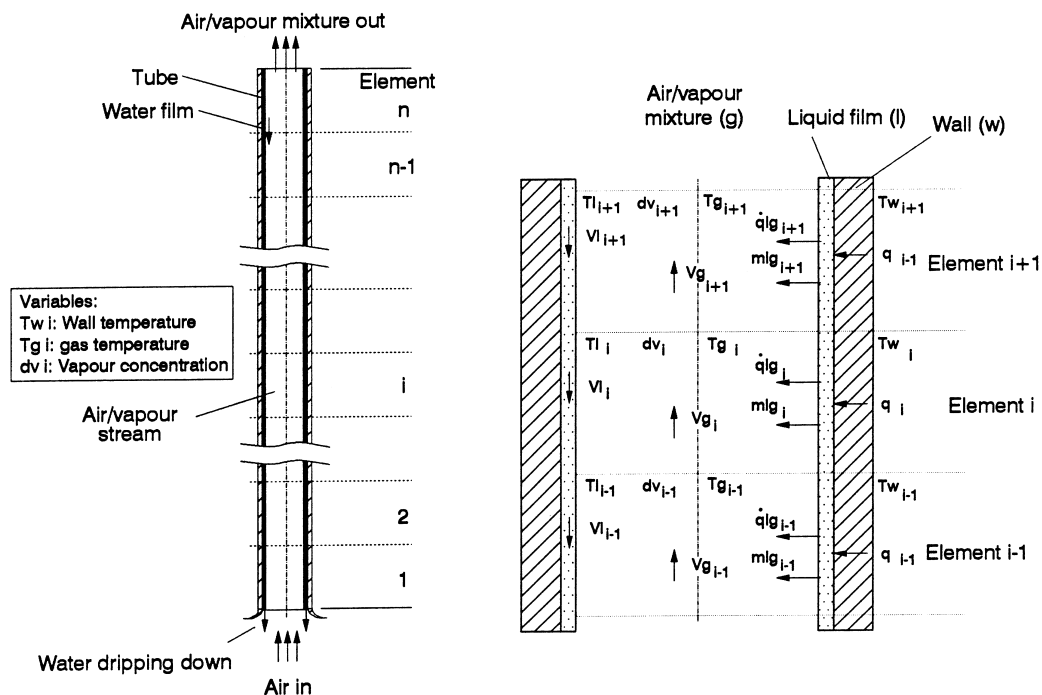


Fig. 9. Modelling details.



element  $n$  the variable  $T_{w,n}$  is obtained and is compared with the boundary condition  $T_{1,n}$ . If the two do not agree to within a specified accuracy, a new value of  $T_{w,0}$  is assumed and the whole calculation is performed again. The process is repeated until the boundary condition  $T_{1,n}$  is satisfied.

Whereas in the dry tests buoyancy influences were very significant and caused impairment of heat transfer under conditions of low air flow rate or high power input, this was not the case with water film cooling. The following semi-empirical equation developed by Jackson and Hall (1979) was used to check that buoyancy influences were small under such conditions.

$$\frac{Nu}{Nu_0} = \left[ 1 - \frac{1500 Gr}{Re^{2.625} Pr^{0.4}} \right]^{0.46}$$

in which  $Nu$  is the Nusselt number under buoyancy-influenced conditions (mixed convection)  $Nu_0$  is the value for buoyancy-free conditions (forced convection), evaluated at the flow rate under consideration.  $Gr$  is Grashof number defined using bulk to wall density difference

$$\left( Gr = \frac{(\rho_b - \rho_w) g D^3}{\rho v^2} \right).$$

3.3. Modelling results and discussion

Figs. 10 and 11 show comparisons between predicted and measured distributions of wall temperature for a power input of 1350 W with water injected at temperatures of 55°C and

70°C, respectively, at a rate of 0.027 kg/s. In each figure, the three sets of experimental data (denoted by markers) correspond to mass flow rates of air through the system of 0.005, 0.010 and 0.015 kg/s. The corresponding wall temperature distributions obtained using the semi-empirical model are shown as lines (full and broken).

Figs. 12 and 13 show further comparisons for power inputs of 3000 and 5000 W with water injected at the rate of 0.027 kg/s at a temperature of 70°C. It can be seen that for a water temperature at inlet of 70°C the model reproduces the observed behaviour extremely well. Quite good agreement was also obtained in the case of experiments with a water temperature at inlet of 55°C. However, agreement between the experimental and predicted results for lower values of water temperature at inlet is less satisfactory. Nevertheless the main trends exhibited by the experimental data were reproduced.

There are three mechanisms involved in the cooling process, namely, laminar convection in the descending water film, evaporation from the water film and turbulent convection of heat in the upward flowing mixture of air and vapour. The model enables us to evaluate separately the contributions to overall heat removal. These are shown in Fig. 14 as a function of water temperature at inlet for a power input of 1350 W.

The upper figure shows the rate of heat removal by convection in the water film. With low water injection temperatures (20°C and 40°C), this is positive, i.e., the falling water film carries heat away with it. For higher water injection temperatures (55°C and 70°C) it becomes negative. The descending water gives up heat and leaves colder than when it was injected.

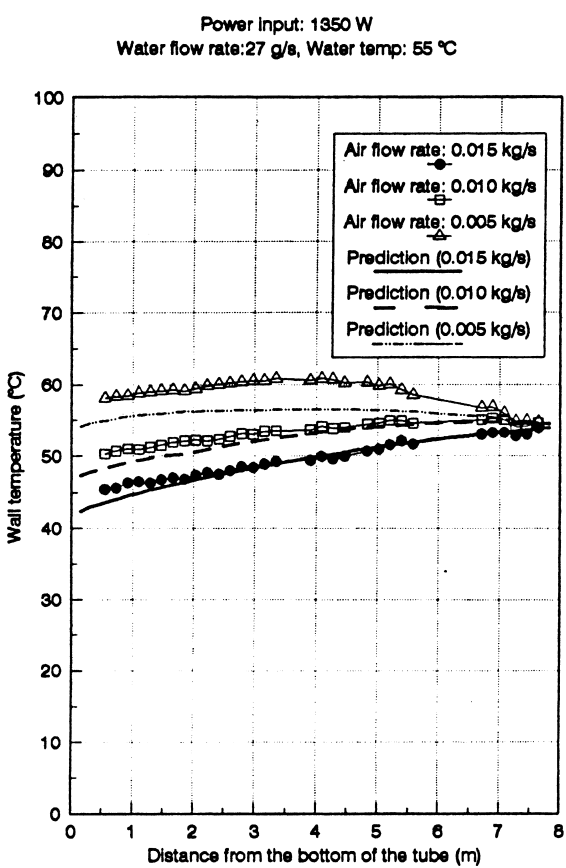


Fig. 10. Comparison of predicted tube wall temperature distributions with experiment.

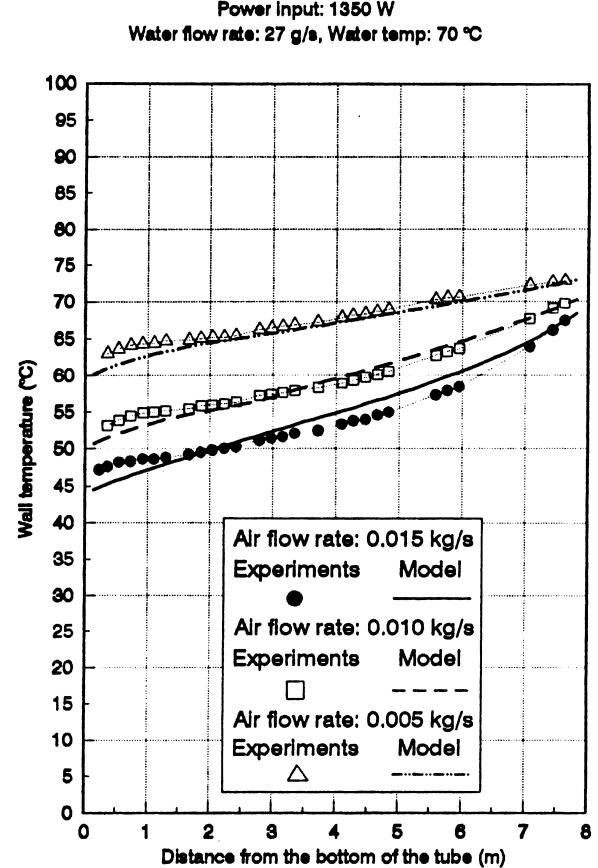


Fig. 11. Comparison of predicted tube wall temperature distributions with experiment.

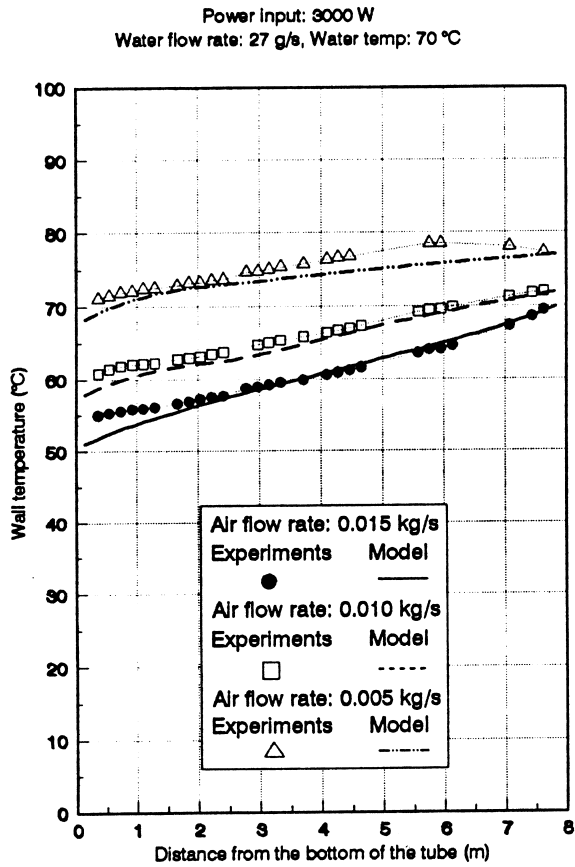


Fig. 12. Comparison of predicted tube wall temperature distributions with experiment.

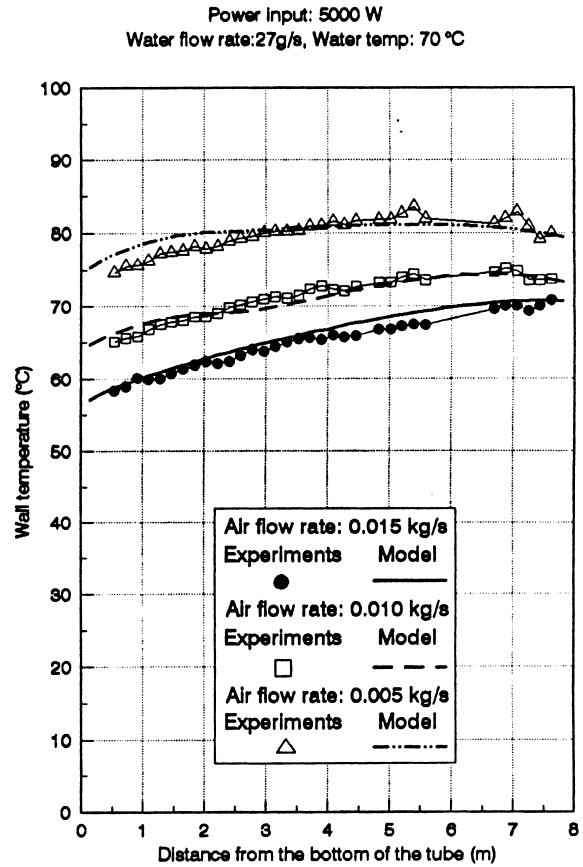


Fig. 13. Comparison of predicted tube wall temperature distributions with experiment.

The lower figure shows separately the rates of heat removal due to evaporation of water from the film and turbulent convection of heat into the mixture of air and vapour. Both increase steadily as the water injection temperature is increased. It can be seen that the rate of heat removal due to evaporation is much higher than that due to turbulent convection into the air/vapour mixture.

Table 1 shows the percentage contributions of the various heat transfer mechanisms for an air flow rate of 0.005 kg/s, a water flow rate of 0.027 kg/s and a power input of 1350 W.

We see that for the lowest water temperature at inlet (20°C), heat transfer by convection in the falling water film accounts for 90% of the overall heat removal. Evaporation from the water film contributes only 9% and turbulent convection of heat into the mixture only 1%. However, this pattern changes dramatically, as the inlet water temperature is increased. For the highest water temperature (70°C), the falling water film does not carry any heat away with it, in fact it releases a considerable amount. Evaporation of water from the falling film is the main mechanism of heat removal and is responsible not only for removing the heat generated in the tube wall but also for cooling down the water which passes through the test section. The contribution of turbulent convection of heat into the air/vapour mixture is much lower (18%).

Fig. 15 shows the predictions of heat removal by the three mechanisms as a function of power input and airflow rate for a water injection rate of 0.027 kg/s and a water temperature at inlet of 70°C. It can be seen that in all cases evaporation of water from the falling film is the dominant mechanisms of heat removal.

#### 4. Conclusions

The experimental and modelling studies reported here have shown that the application of water film cooling substantially reduces tube wall temperatures in comparison with those for cooling by airflow alone. Three mechanisms are involved: (a) laminar convection in the descending water film, (b) turbulent convection of heat into the upward flowing mixture of air and vapour, and (c) evaporation of water from the water film into the air/vapour mixture. With water injection at the two higher temperatures used in the tests (55°C and 70°C) evaporation is the dominant mechanism for heat removal. In contrast, with water injection at the lowest (20°C), the principal cooling mechanism is laminar convection in the descending water film. The simple semi-empirical model used in this study to simulate

Table 1  
Percentage of the heat generated which is removed by (a) laminar convection in the falling water film, (b) turbulent convection of heat in the air/vapour mixture and (c) evaporation from the water film

Water inlet temp. (°C)	Laminar convection in falling water film (%)	Turbulent convection of heat into mixture (%)	Evaporation from the water film (%)
20	90	1	9
40	43	9	48
55	-5	12	93
70	-117	18	199

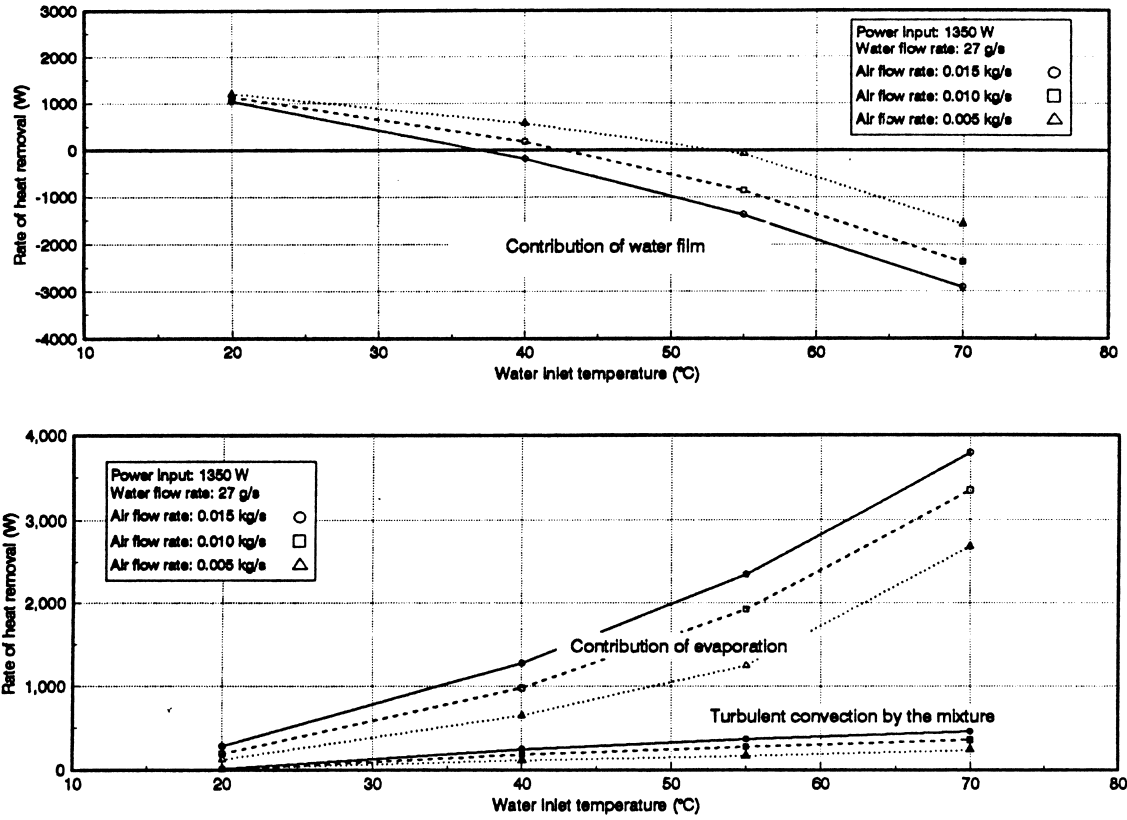


Fig. 14. Contributions of heat transfer mechanisms.

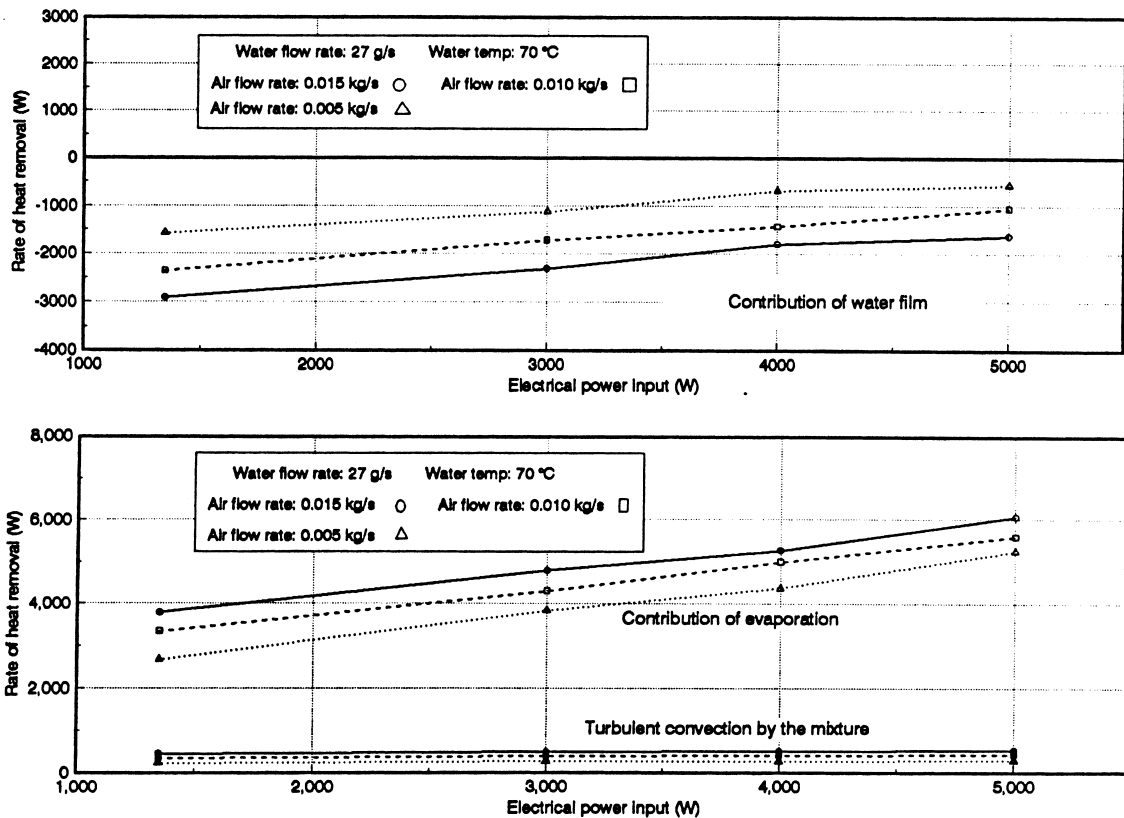


Fig. 15. Contributions of heat transfer mechanisms.

the experiments has enabled a useful picture to be obtained of the extent to which the various mechanisms of heat transfer involved in the cooling process contribute to the removal of heat in the situation considered.

### Acknowledgements

Financial support for the work reported here was provided by AEA Technology under the terms of a research contract funded by the DTI under the General Nuclear Safety Research Programme. The authors gratefully acknowledge the help provided by J.L. Diez and F.R. Garcia in the experimental work.

### References

- Burschi, H.J., Vijuk, R.P., 1991. AP-600 plant design-meet industry needs. *The Nuclear Engineer* 32 (5), 155–161.
- He, S., An, P., Li, J., Jackson, J.D., 1998. Combined heat and mass transfer in a uniformly heat vertical tube with water film cooling. Proceedings. 11th Turbulent Shear Flow Symposium, Grenoble.
- Jackson, J.D., Hall, W.B., 1979. Influences of buoyancy on heat transfer to fluids flowing the vertical tube under turbulent conditions. In: *Turbulent Forced Convection in Channels and Bundles*, vol. 2, Advanced Study Institute Book, (Hemisphere, Washington DC, pp. 613–640.
- Jackson, J.D., Cotton, M.A., Axcell, B.P., 1989. Review: Studies of mixed convection in vertical tubes. *International Journal of Heat and Fluid Flow* 10, 2–15.
- Jackson, J.D., Li, J., Poskas, P., 1995. Comparison of forced and passive heat removal by air flowing upwards inside a heated vertical passage. In: *I. Mech. E. Conference Transactions, Fourth UK National Heat Transfer Conference on Heat Transfer, C510/131/95*, pp. 243–247.
- Li, J. 1994. Studies of buoyancy-influenced convective heat transfer to air in a vertical tube, Ph.D. Thesis, University of Manchester.
- Petukhov, B.S., Kurganov, V.A., Gladuntsov, A.I., 1972. Turbulent heat transfer in tubes to gases with variable physical properties. *Heat and Mass Transfer* 1, 117–127, Izd. ITMO AN BSSR, Minsk (in Russian).
- Ueda, T., Tanaka, H., 1975. Measurement of velocity, temperature and velocity fluctuation distributions in liquid films. *International Journal of Multiphase Flow* 2, 261–272.